Journal of Applied Physics ARTICLE scitation.org/journal/jap

Origin and anomalous behavior of dominant defects in 4H-SiC studied by conventional and Laplace deep level transient spectroscopy

Cite as: J. Appl. Phys. **127**, 064503 (2020); doi: 10.1063/1.5140731
Submitted: 2 December 2019 · Accepted: 26 January 2020 ·
Published Online: 11 February 2020

Ł. Gelczuk,[1,a)] M. Dąbrowska-Szata,[1] Vl. Kolkovsky,[2] M. Sochacki,[3] J. Szmidt,[3] and T. Gotszalk[1]

AFFILIATIONS

[1]Faculty of Microsystem Electronics and Photonics, Wrocław University of Science and Technology, Janiszewskiego 11/17, 50-372 Wroclaw, Poland
[2]Technische Universität Dresden, 01062 Dresden, Germany
[3]Institute of Microelectronics and Optoelectronics, Warsaw University of Technology, Koszykowa 75, Warsaw 00-662, Poland

Note: This paper is part of the Special Topic on Defects in Semiconductors 2020.
[a)]**Author to whom correspondence should be addressed:** lukasz.gelczuk@pwr.edu.pl

ABSTRACT

Several deep level defects were observed by conventional deep level transient spectroscopy (DLTS) and high-resolution Laplace DLTS (LDLTS) in n-type 4H-SiC junction barrier Schottky diodes. We have shown that the broad DLTS peak labeled $Z_{1/2}$ has, in fact, two components, Z_1 and Z_2, with activation enthalpies for electron emission of 0.63 eV and 0.68 eV, respectively. The reorientation process between these two components was observed. A combination of double-correlated DLTS and LDLTS demonstrated an anomalous reduction of the emission rate and an increase of the activation enthalpy of Z_2 with an increase of the reverse bias applied to the diode. The possible explanation of this phenomenon could be correlated with a tensile stress in epitaxial SiC layers. The results observed are discussed in the frame of the model that correlates Z_1 and Z_2 with carbon vacancies (V_C), located at hexagonal (h) and cubic (k) lattice sites, respectively. We also discussed the origin of other traps E_0–E_5 with particular emphasis on a N-related shallow donor level located at 0.04 eV below the conduction band, which has never been previously reported by DLTS studies.

I. INTRODUCTION

Silicon carbide (SiC) has great potential for realizing high-power, high-temperature, and high-frequency operating devices. Among technologically feasible SiC polytypes, hexagonal 4H-SiC is considered as the most suitable choice for such device applications because of its large bandgap, high breakdown field, high thermal conductivity, and also higher electron and hole mobility as compared to the 6H polytype.[1,2] The presence of unintentionally introduced defects can significantly affect the performance of SiC devices and effectively limits their full-scale commercialization. Besides shallow dopants, intrinsic and extrinsic defects giving rise to deep energy levels in the bandgap of SiC were often reported.[3,4] Deep level defects can act either as electron or hole traps, thereby reducing the conductivity of the material or generation–recombination centers limiting a carrier's lifetime.[5] Structural defects in SiC, such as dislocations or micropipes, can also evoke barrier height inhomogeneities and an increase in the leakage current of Schottky barrier diodes (SBDs).[6,7]

Different defects have been already reported in bulk and epitaxial 4H-SiC layers grown by different techniques.[3,4] Among them, a defect labeled $Z_{1/2}$ with an activation enthalpy of around 0.6–0.7 eV below the conduction band is almost always dominant in 4H-SiC samples. $Z_{1/2}$ acts as a strong lifetime killer and its origin has been discussed in Refs. 8–27. Different models were suggested to describe the structure of this defect. It seems very likely that $Z_{1/2}$ is correlated with an isolated vacancy of carbon (V_C) or a complex, which contains V_C. This assignment is mainly based on the correlation of a deep level transient spectroscopy (DLTS) peak corresponding to $Z_{1/2}$ with paramagnetic resonance (EPR) measurements.[13,20] The correlation of $Z_{1/2}$ with a carbon

vacancy is also consistent with a significant increase in the concentration of this defect after electron irradiation with a low energy of 100–200 keV, which corresponds to the threshold energy displacing primarily C atoms in SiC and creating defects in the C sublattice.[18,19] This model was also in good agreement with a lower concentration of this defect observed in SiC epitaxial layers grown under C-rich conditions.[26]

One should emphasize that the DLTS peak corresponding to $Z_{1/2}$ consists of two defects, which could be reliably resolved by high-resolution Laplace DLTS (LDLTS). Recently, by combining Laplace DLTS measurements and theoretical calculations, Capan *et al.*[23] showed that different components of $Z_{1/2}$ (Z_1 and Z_2) could belong to double-negatively charged acceptor states of V_C located at hexagonal (h) and cubic (k) lattice sites of 4H-SiC. However, the charge state of the defect has never been straightforwardly determined. The information about the charge state of defects can be directly obtained from the analysis of the dependence of their emission rates on the electrical field applied to the diode. The logarithm of the emission rate of a defect with the Coulomb potential should exhibit the square root dependence on the electric field. In some cases, even defects with the Coulomb potential do not exhibit such a dependence, as described for EL2 in Ref. 28. The results investigating a field dependence of $Z_{1/2}$ are controversial. No enhancement of the emission rate of $Z_{1/2}$ has been observed in Refs. 17, 29, and 30, and the authors concluded its acceptorlike behavior. In contrast, Evwaraye *et al.*[31] detected a strong enhancement of the emission rate of this defect with the electric field, and the authors described this enhancement with a phonon assisted tunneling mechanism with two tunneling stages, resulting from the difference in the tunneling time from the Z_1 and Z_2 defects. In contrast, Fang *et al.*[11] reported a donorlike behavior of Z_1 after the correlation of Hall-effect measurements with DLTS.

Both Z_1 and Z_2 exhibit the negative-U properties as reported in Refs. 20, 21, and 23. Their metastable states were observed by applying DLTS or Laplace DLTS with very short filling pulses (around ns) at around 250 K.

Besides $Z_{1/2}$, nitrogen (N)-related defects were often reported in 4H-SiC.[32] Nitrogen (N) is usually used as the main impurity for the n-type doping of different SiC polytypes and it should introduce shallow donor levels in the upper part of the bandgap.[32] By using admittance spectroscopy and Hall-effect measurements, two different defects with an activation enthalpy of 0.045–0.065 eV for donors at hexagonal lattice site N(h) and 0.105–0.125 eV for donors at cubic lattice site N(k) were observed.[32,33] However, these defects have never been reported by DLTS measurements.

In comparison to $Z_{1/2}$, the concentration of other unintentionally introduced defects observed in 4H-SiC is significantly lower, and they do not act as strong recombination/generation centers in 4H-SiC.

The goal of the present study is twofold. First of all, we would like to shed light on the origin of $Z_{1/2}$ by comprehensive studies of conventional DLTS[34] and high-resolution Laplace DLTS[35] including field effect measurements. Second, we concentrate our attention on N-related donors in N-doped 4H-SiC. We will show that N indeed introduces donor levels with an activation enthalpy of around 0.04 eV, which could be also observed by conventional DLTS measurements at low temperatures.

II. EXPERIMENT

10 μm thick 4H-SiC epitaxial layers grown by a Aixtron/Epigress VP508 horizontal hot-wall reactor on a 350 μm thick n-type 4H-SiC substrate with a net donor concentration of about 5×10^{18} cm^{-3} were investigated. These epitaxial layers were N doped and had a typical concentration of about 1.5×10^{16} cm^{-3}. Aluminum ion (Al^+) implantation was performed to form junction termination extensions around the Schottky contacts and ultimately to produce junction barrier Schottky (JBS) diodes. Further details of the growth and post-growth procedures in manufacturing JBS diodes are described in Ref. 36. For electrical characterization, a 150 nm thick titanium (Ti) layer was deposited on a backside of the wafer by the magnetron sputtering technique. Afterward, the layers were annealed at 1000 °C for 3 min in argon (Ar) atmosphere and covered with a 1 μm thick gold (Au) film in order to form ohmic contacts. The Schottky contacts, with an area of 0.26 mm^2, were made by deposition of 200 nm thick nickel (Ni) on the epitaxial layer side by magnetron sputtering and following annealing in Ar atmosphere at 350 °C for 5 min.

The quality of JBS diodes was investigated by temperature dependent current–voltage (I–V) and capacitance–voltage (C–V) measurements by using a Keithley 2601A source-meter and a Boonton 7200 capacitance bridge. The diodes exhibit a low reverse leakage current of about 0.2 nA at a reverse bias of −10 V. A Schottky barrier height of 1.21 ± 0.05 eV, an ideality factor of 1.1 ± 0.1, a series resistance of 63–73 Ω, and a doping concentration of 1.65×10^{16} cm^{-3} was extracted in a 4H-SiC epilayer from I–V and C–V characteristics at 300 K.[36] For DLTS and Laplace DLTS measurements, the samples were mounted on a cold finger in a helium (He) closed cycle refrigerator, allowing the measurements from 15 K to 350 K or in a liquid nitrogen (LN_2) cryostat with a temperature range of 80 K–480 K. These measurements were performed with a different reverse bias (V_R) varying from −10 V to −2 V and a constant filling pulse voltage (V_P), in a temperature range of 20–480 K. A width of the filling pulse was 1 ms. In order to obtain thermal activation enthalpy (E_a) and apparent capture cross section (σ_a), different emission rate windows (RWs) in a range of 5 s^{-1}–2000 s^{-1} were used. The concentration and the field effect measurements were performed by using the double-correlated DLTS (DDLTS) and the Laplace DLTS techniques with two filling pulses. Capacitance transients were recorded in a range of 315 K–350 K with a temperature stability of ±0.02 K.

III. RESULTS

Figure 1 presents a typical DLTS spectrum recorded in n-type 4H-SiC JBS diodes. The broad and asymmetric peak, labeled $Z_{1/2}$, with a maximum at about 322 K at a rate window of 50 s^{-1} dominates this spectrum. Besides this dominant DLTS peak, several weaker peaks, labeled E_0–E_5, were also observed at lower temperatures of about 33 K, 93 K, 121 K, 156 K, 185 K, 247 K, respectively. Positive DLTS signals indicate that all peaks are correlated with the thermal emission of majority carriers from deep levels.

The electrical parameters of the defects shown in Fig. 1 such as activation enthalpy (E_a) and apparent capture cross section (σ_a) were obtained from the Arrhenius plot and are combined in

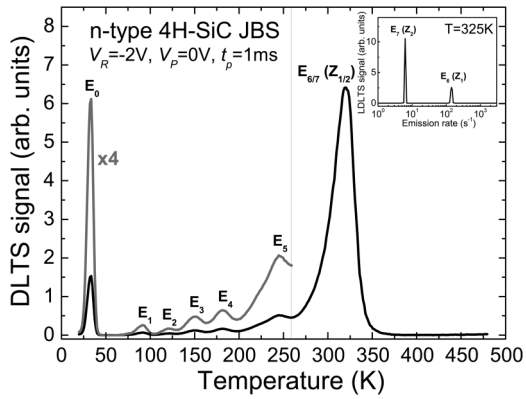

FIG. 1. Conventional DLTS spectra of n-type 4H-SiC JBS diodes recorded in a temperature range of 20–480 K with a rate window (RW) of 50 s^{-1}. The measurement conditions are given in the figure. The inset shows a high-resolution Laplace DLTS spectrum recorded at 325 K.

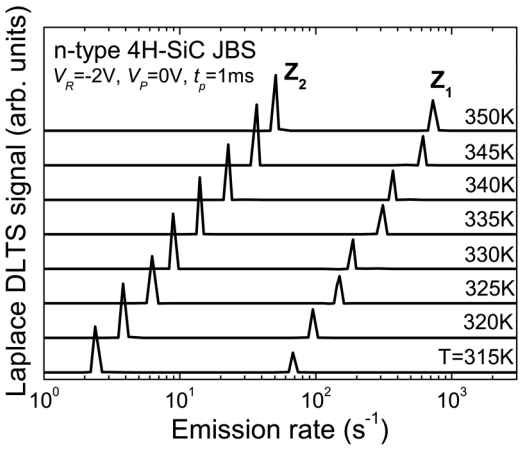

FIG. 2. High-resolution Laplace DLTS spectra of n-type 4H-SiC JBS diodes recorded in a temperature range of 315–350 K.

Table I. In addition, Table I contains the information about the concentration of the defects. The method for determining deep trap parameters by DLTS can be found in the supplementary material.

In order to check whether the $Z_{1/2}$ peak contains different components Z_1 and Z_2, which cannot be resolved by the conventional DLTS technique, we applied the high-resolution Laplace DLTS technique. An exemplary Laplace DLTS spectrum, obtained at 325 K, is shown in the inset of Fig. 1. Figure 2 shows Laplace DLTS spectra recorded with a reverse bias of −2 V and one filling pulse of 0 V at different temperatures varying in the range of 315–350 K. In good agreement with previous studies, two delta-peaks labeled Z_1 and Z_2 were observed in these spectra. Z_1 was observed at higher emission rates and we correlate this peak with the low-temperature shoulder of $Z_{1/2}$ observed in Fig. 1. The amplitude of Z_2 is significantly larger than that of Z_1. However, the ratio between the concentration of Z_1 and Z_2 is not constant. It increases by increasing the temperature, whereas the sum of these defects remains approximately constant.

The activation enthalpy and apparent capture cross section of Z_1 and Z_2 were determined from the Arrhenius plots (Fig. 3) and they are collected in Table II. The concentration of these defects obtained from Laplace DLTS measurements is also combined in this table.

In order to shed light on the charge state of the defects, we analyzed the enhancement of their emission rates as a function of electric field. By using the double-correlated DLTS (DDLTS) technique, we detected the shift of the dominant DLTS peak $Z_{1/2}$ toward a higher temperature by increasing the reverse bias applied

TABLE I. Electrical parameters of deep electron traps obtained in 4H-SiC JBS diodes from DLTS measurements, i.e., activation enthalpy ($E_a = E_C - E_T$), apparent electron capture cross section (σ_a), and defect concentration (N_T). In the last two columns, a possible attribution of the traps is presented.

Trap	E_a (eV)	σ_a (cm^2)	N_T (cm^{-3})	Deep level	Possible attribution
E_0	0.04 ± 0.02	$1.8 \pm 0.3 \times 10^{-17}$	$3.4 \pm 0.04 \times 10^{15}$	N(k)[a–c]	Impurity defect
E_1	0.13 ± 0.02	$2.1 \pm 0.4 \times 10^{-16}$	$8.6 \pm 0.02 \times 10^{13}$	Ti(h)[a,b,d]	Impurity defect
E_2	0.18 ± 0.02	$1.4 \pm 0.4 \times 10^{-16}$	$5.1 \pm 0.04 \times 10^{13}$	Ti(k)[a,b,d]	Impurity defect
E_3	0.23 ± 0.03	$1.6 \pm 0.4 \times 10^{-16}$	$1.4 \pm 0.03 \times 10^{14}$	SE2[e]	Single plain SF
E_4	0.33 ± 0.04	$2.9 \pm 0.5 \times 10^{-15}$	$1.9 \pm 0.05 \times 10^{14}$	ID_4[b], P3[b]	Intrinsic defect
E_5	0.45 ± 0.04	$1.1 \pm 0.3 \times 10^{-15}$	$3.2 \pm 0.06 \times 10^{14}$	ID_8[b], EH1[f]	Intrinsic defect
$E_{6/7}$	0.68 ± 0.03	$9.7 \pm 0.4 \times 10^{-15}$	$4.5 \pm 0.1 \times 10^{15}$	$Z_{1/2}$[a–e]	Intrinsic defect

[a]Reference 3.
[b]Reference 4.
[c]Reference 33.
[d]Reference 38.
[e]Reference 37.
[f]Reference 18.

TABLE II. Electrical parameters of Z_1 and Z_2 estimated from Laplace DLTS measurements, i.e., activation enthalpy ($E_a = E_C - E_T$), apparent electron capture cross section (σ_a), and defect concentration (N_T).

Trap	E_a (eV)	σ_a (cm^2)	N_T (cm^{-3})
Z_1	0.63 ± 0.02	$7.5 \pm 0.2 \times 10^{-15}$	$1.4 \pm 0.05 \times 10^{15}$
Z_2	0.68 ± 0.02	$1.2 \pm 0.3 \times 10^{-14}$	$5.7 \pm 0.05 \times 10^{15}$

to the diode and keeping two filling pulses at 0 V and −1 V (Fig. 4). Laplace DLTS measurements further support these findings: the emission rate of Z_2 was significantly reduced by applying the higher reverse bias to the diode (Fig. 5). In contrast, Z_1 was only observed at lower values of the reverse bias. This is inconsistent with DLTS measurements, where the low-temperature shoulder of $Z_{1/2}$ was also observed at higher reverse biases and we will discuss this observation below. A similar shift of DLTS peaks toward high temperatures with increasing electric field was also observed for minor peaks E_1–E_5.

Figure 6 exhibits the Arrhenius plots recorded for the dominant peak Z_2 by applying different reverse biases to the diode by using Laplace DLTS measurements. As one can see from the figure, the activation enthalpy increases by increasing the reverse bias applied to the diode.

IV. DISCUSSION

Preliminary results describing DLTS spectra in n-doped 4H-SiC and possible identification of the traps E_1–$E_{6/7}$ have been already previously reported in Ref. 36. Nevertheless, we also discuss the assignment of the peaks with some extension in the present study. By comparing the electrical properties of the traps observed in Fig. 1 with those in the literature, one can correlate them with the following defects.

E_0 has never been previously detected by DLTS measurements in 4H-SiC. However, the activation enthalpy of this defect is close to those reported for N-related donors [N(h) and N(k)] in Ref. 33. The relatively high concentration of E_0 (around 3.4×10^{15} cm^3) further confirms its attribution to N-related defects, since the 4H-SiC layers were intentionally doped with N. In addition, this defect has never been observed in 4H-SiC samples without N.[33] On the basis of these findings, we assign E_0 to N(k) since the N(h) donors are located closer to the conduction band, and they are probably responsible for n-type doping in SiC.

E_1 and E_2 with an activation enthalpy of about E_C—0.13 eV and E_C—0.18 eV were previously attributed to Ti atoms at hexagonal (h) and cubic (k) positions in the lattice, respectively.[38] This assignment is in good agreement with our results. The concentrations of E_1 and E_2 obtained in the present study are about $5–8 \times 10^{13}$ cm^{-3} and they are typical for Ti in SiC.[38] This is due to the fact that transition metal impurities, e.g., titanium, are

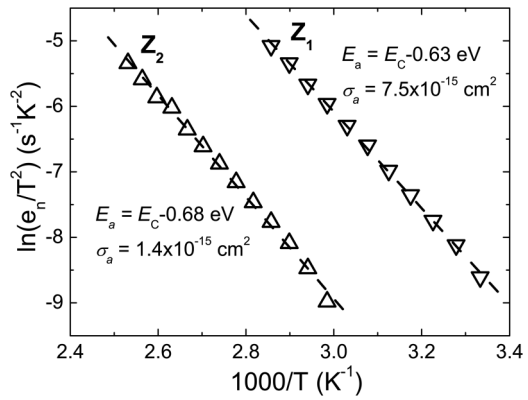

FIG. 3. Arrhenius plots of electron emission rates of Z_1 and Z_2 in n-type 4H-SiC JBS diodes. The dashed lines represent the best least-squares fitting to the experimental data.

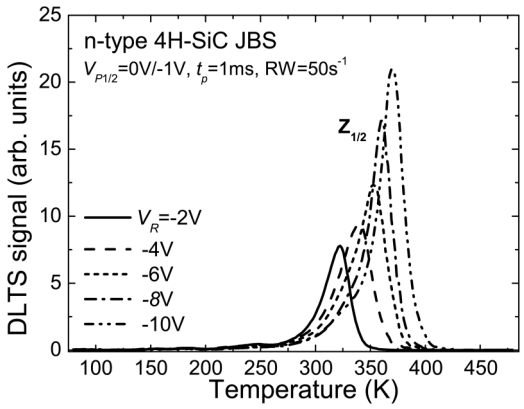

FIG. 4. Double-correlated DLTS spectra of n-type 4H-SiC JBS diodes measured as a function of reverse bias (V_R) with two filling pulses (V_{P1}, V_{P2}).

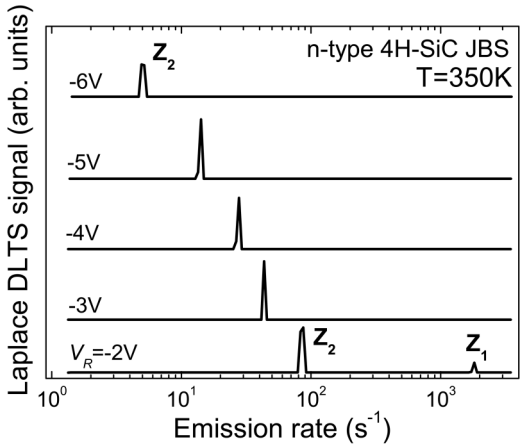

FIG. 5. Laplace DLTS spectra of n-type 4H-SiC JBS diodes recorded at 350 K for different reverse biases (V_R) and two filling pulses $V_{P1} = 0$ V and $V_{P2} = -1$ V, rate window of 50 s^{-1}, and a width of the filling pulse of 1 ms.

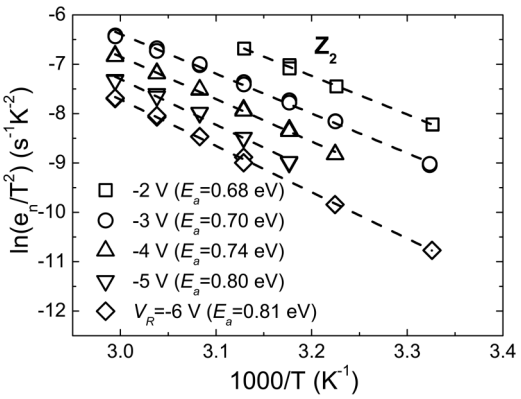

FIG. 6. Arrhenius plots of electron emission rates of Z_2 in n-type 4H-SiC JBS diodes for the same measurement conditions as in Fig. 5. The dashed lines represent the best least-squares fitting to the experimental data.

dominant background impurities present in graphite parts used in SiC growth reactors for sublimation and epitaxy. In spite of evaporation of Ti on the backside of our samples, it is very unlikely that this could lead to any Ti contamination in the depletion region of diodes even after annealing at 1000 °C. Danno *et al.*[39] demonstrated that the diffusivity of Ti should be still negligible at such temperatures in 4H-SiC.

The activation enthalpy of E_3 (around E_C—0.23 eV) is very similar to that of the electron trap SE2 reported previously in Ref. 37. This trap was observed in different SiC structures (i.e., simple Schottky diodes as well as p+/n diodes with and without JTEs) and it was attributed to a single plain stacking fault (SF).[40]

The origin of E_4 (E_C—0.33 eV) and E_5 (E_C—0.45 eV) is not clear until now. However, their electrical properties are similar to ID_4 (P3)[4] and ID_8 (EH1),[4,18] respectively, and we tentatively attribute these defects to some intrinsic defects in 4H-SiC.[36]

In good agreement with the previous studies, we showed that $Z_{1/2}$ consists of two components Z_1 (E_C—0.63 eV) and Z_2 (E_C—0.68 eV), which could be resolved by high-resolution Laplace DLTS. The ratio between the concentration of Z_1 and Z_2 was around 1:4, and it is slightly different from that observed in Refs. 22 and 23, where the authors also resolved the peaks by the Laplace DLTS technique. The discrepancy observed in different studies can be explained by different growth conditions, thermal history, and/or doping parameters of the samples. In Refs. 22 and 23, Z_1 and Z_2 were assigned to the $Z_1(=/0)$ and $Z_2(=/0)$ transitions of $V_C(h)$ and $V_C(k)$, and this assignment is also consistent with our results. In this case, one can also explain different concentrations of Z_1 and Z_2 by the lower formation energy of V_C located at the *k*-site in comparison to that located at the *h*-site.[41]

In Refs. 21 and 23, the negative-U properties of Z_1 and Z_2 were reported by applying short filling pulses during DLTS or Laplace DLTS measurements. Such conditions are essential to ensure that the number of electrons in the depletion region is not high enough to fill the traps with two electrons and only a single acceptor state could be detected. Unfortunately, we were not able to confirm the negative-U ordering of these levels probably due to the overlapping of the metastable peaks with E_5, which is also located at around 240–250 K.

As mentioned in Sec. I, information about the charge states of defects can be obtained from the dependence of their emission rate on the electric field. Usually, defects with the Coulomb potential exhibit the enhancement of the logarithm of their emission rate as a function of the square root of the electric field. In contrast, we observed the reduction of the emission rate of Z_2 with increasing reverse bias applied to the diode. Epitaxial SiC layers are known to have a tensile residual stress due to the mismatch in the lattice constant and thermal expansion coefficients.[42] The values of the stress in epitaxial films can reach even more than 700–1000 MPa, and they depend on the thickness of the layers. Such a stress may induce a shift of the emission rate of defects or even lead to a splitting of the related Laplace DLTS lines into a characteristic pattern according to the point symmetry of these defects. Furthermore, it can be even more complicated since the stress might be nonuniform in epitaxial SiC layers. In this case, the average emission rates of Z_1 and Z_2 should be determined by Laplace DLTS measurements, and this can lead to the broadening of Laplace DLTS peaks. 4H-SiC is a piezoelectric material.[43] The piezoelectric effect describes the generation of a charge or voltage by applying the stress to a crystal and it is usually reversible. Then, by applying an external electric field, one can modify the stress in 4H-SiC epitaxial layers, resulting in a shift of the emission rates of the defects. In support of this model, an anomalous shift of the emission rate was also observed for other defects E_1–E_5 by applying different biases.

We interpret the absence of Z_1 in Laplace DLTS spectra recorded at higher reverse voltages than −2 V with the reorientation of this defect at such a high temperature. The Laplace DLTS spectra were recorded at significantly higher temperatures in comparison to the low-temperature shoulder of $Z_{1/2}$ observed in DLTS spectra (Fig. 4). The reorientation process between Z_1 and Z_2 is also confirmed by Laplace DLTS measurements presented in Fig. 2. As mentioned above, the ratio between the concentrations of Z_1 and Z_2 increases by increasing the measurement temperatures, whereas their sum remains approximately constant. The reorientation between Z_1 and Z_2 supports further that the defects are very likely to have a similar structure. However, further studies are necessary for better understanding of this reorientation process in detail.

V. CONCLUSIONS

Several deep level defects were detected by DLTS and Laplace DLTS in 4H-SiC. We showed that the broad DLTS peak labeled $Z_{1/2}$ consisted of two deep level defects, Z_1 and Z_2, with close electron emission rate and activation enthalpy 0.63 eV and 0.68 eV, respectively. From the Laplace DLTS measurements, the reorientation between Z_1 and Z_2 was observed. This reorientation supports further the attribution of the two components of the $Z_{1/2}$ center to carbon vacancies (V_C), located at hexagonal (*h*) and cubic (*k*) lattice sites in 4H-SiC. A combination of double-correlated DLTS and Laplace DLTS measurements enabled us to detect the unusual behavior of the emission rate of Z_2 with electric field. The possible explanation of this phenomenon was correlated with a tensile residual stress in the 4H-SiC epitaxial layers. Besides Z_1 and Z_2, several

other electron traps E_0–E_5 were also detected in this material. We reported the electrical properties of these defects and discussed their origin with a particular emphasis on a N-related shallow donor level located at 0.04 eV below the conduction band.

SUPPLEMENTARY MATERIAL

See the supplementary material for details about the determination of deep level trap parameters in the studied 4H-SiC JBS diodes on the basis of DLTS temperature spectra and Arrhenius plots.

ACKNOWLEDGMENTS

This work was supported by the Wrocław University of Science and Technology statutory grant.

REFERENCES

[1]P. G. Neudeck and S. Technology, in *The VLSI Handbook*, 2nd ed., edited by W.-K. Chen (Florida CRC Press, Boca Raton, 2007), pp. 5.1–5.3.
[2]B. J. Baliga, *Power Semiconductor Devices* (PWS Publishing Company, Boston, 1999).
[3]A. A. Lebedev, Semiconductors **33**, 107 (1999).
[4]T. Dalibor, G. Pensl, H. Matsunami, T. Kimoto, W. J. Choyke, A. Schöner, and N. Nordell, Phys. Status Solidi A **162**, 199 (1997).
[5]P. B. Klein, Phys. Status Solidi A **206**, 2257 (2009).
[6]D. J. Ewing, Q. Wahab, R. R. Ciechonski, M. Syvajarvi, R. Yakimova, and L. M. Porter, Semicond. Sci. Technol. **22**, 1287 (2007).
[7]Ł. Gelczuk, P. Kamyczek, E. Popko, and M. Dąbrowska-Szata, Solid-State Electron. **99**, 1 (2014).
[8]I. Pintilie, L. Pinitilie, K. Irmscher, and B. Thomas, Appl. Phys. Lett. **81**, 4841 (2002).
[9]T. A. G. Eberlein, R. Jones, and P. R. Briddon, Phys. Rev. Lett. **90**, 225502 (2003).
[10]L. Storasta, A. Henry, P. Bergman, and E. Janzén, Mater. Sci. Forum **457–460**, 469 (2004).
[11]Z.-Q. Fang, D. C. Look, A. Saxler, and W. C. Mitchel, Phys. B Condens. Matter **308–310**, 706 (2001).
[12]K. Danno, T. Kimoto, and H. Matsunami, Appl. Phys. Lett. **86**, 122104 (2005).
[13]K. Kawahara, X. Thang Trinh, N. Tien Son, E. Janzén, J. Suda, and T. Kimoto, Appl. Phys. Lett. **102**, 112106 (2013).
[14]P. B. Klein, B. V. Shanabrook, S. W. Huh, A. Y. Polyakov, M. Skowronski, J. J. Sumakeris, and M. J. O'Loughlin, Appl. Phys. Lett. **88**, 052110 (2006).
[15]K. Danno, D. Nakamura, and T. Kimoto, Appl. Phys. Lett. **90**, 202109 (2007).
[16]A. Kawasuso, F. Redmann, R. Krause-Rehberg, M. Weidner, T. Frank, G. Pensl, P. Sperr, W. Triftshäuser, and H. Itoh, Appl. Phys. Lett. **79**, 3950 (2001).
[17]A. Castaldini, A. Cavallini, and L. Rigutti, Semicond. Sci. Technol. **21**, 724 (2006).
[18]L. Storasta, J. P. Bergman, E. Janzén, A. Henry, and J. Lu, J. Appl. Phys. **96**, 4909 (2004).
[19]K. Danno and T. Kimoto, J. Appl. Phys. **100**, 113728 (2006).
[20]N. T. Son, X. T. Trinh, L. S. Løvlie, B. G. Svensson, K. Kawahara, J. Suda, T. Kimoto, T. Umeda, J. Isoya, T. Makino, T. Ohshima, and E. Janzén, Phys. Rev. Lett. **109**, 187603 (2012).
[21]C. G. Hemmingsson, N. T. Son, A. Ellison, J. Zhang, and E. Janzén, Phys. Rev. B **58**, R10119 (1998).
[22]I. Capan, T. Brodar, Ž Pastuović, R. Siegele, T. Ohshima, S. Sato, T. Makino, L. Snoj, V. Radulović, J. Coutinho, V. J. B. Torres, and K. Demmouche, J. Appl. Phys. **123**, 161597 (2018).
[23]I. Capan, T. Brodar, J. Coutinho, T. Ohshima, V. P. Markevich, and A. R. Peaker, J. Appl. Phys. **124**, 245701 (2018).
[24]G. Alfieri, E. V. Monakhov, B. G. Svensson, and M. K. Linnarsson, J. Appl. Phys. **98**, 043518 (2005).
[25]H. M. Ayedh, R. Nipoti, A. Hallén, and B. G. Svensson, Appl. Phys. Lett. **107**, 252102 (2015).
[26]T. Kimoto, S. Nakazawa, K. Hashimoto, and H. Matsunami, Appl. Phys. Lett. **79**, 2761 (2001).
[27]J. Zhang, L. Storasta, J. P. Bergman, N. T. Son, and E. Janzén, J. Appl. Phys. **93**, 4708 (2003).
[28]W. R. Buchwald and N. M. Johnson, J. Appl. Phys. **64**, 958 (1988).
[29]T. Dalibor, G. Pensl, T. Kimoto, H. Matsunami, S. Sridhara, R. P. Devaty, and W. J. Choyke, Diam. Relat. Mater. **6**, 1333 (1997).
[30]J. P. Doyle, M. K. Linnarsson, P. Pellegrino, N. Keskitalo, B. G. Svensson, A. Schöner, N. Nordell, and J. L. Lindström, J. Appl. Phys. **84**, 1354 (1998).
[31]A. O. Evwaraye, S. R. Smith, W. C. Mitchel, and G. C. Farlow, J. Appl. Phys. **106**, 063702 (2009).
[32]W. Götz, A. Schöner, G. Pensl, W. Suttrop, W. J. Choke, R. Stein, and S. Leibenzeder, J. Appl. Phys. **73**, 3332 (1993).
[33]T. Kimoto, A. Itoh, H. Matsunami, S. Sridhara, L. L. Clemen, R. P. Devaty, W. J. Choyke, T. Dalibor, C. Peppermüller, and G. Pensl, Appl. Phys. Lett. **67**, 2833 (1995).
[34]D. V. Lang, J. Appl. Phys. **45**, 3023 (1974).
[35]L. Dobaczewski, A. R. Peaker, and K. Bonde Nielsen, J. Appl. Phys. **96**, 4689 (2004) and references therein.
[36]Ł. Gelczuk, M. Dąbrowska-Szata, M. Sochacki, and J. Szmidt, Solid State Electron. **94**, 56 (2014).
[37]F. Fabbri, D. Natalini, A. Cavallini, T. Sekiguchi, R. Nipoti, and F. Moscatelli, Superlatt. Microstruct. **45**, 383 (2009).
[38]T. Dalibor, G. Pensl, N. Nordell, and A. Schöner, Phys. Rev. B **55**, 13618 (1997).
[39]K. Danno, H. Saitoh, A. Seki, T. Shirai, H. Suzuki, T. Bessho, Y. Kawai, and T. Kimoto, Appl. Phys. Express **5**, 031301 (2012).
[40]M. Skowronski and S. Ha, J. Appl. Phys. **99**, 011101 (2006).
[41]J. Coutinho, V. J. B. Torres, K. Demmouche, and S. Öberg, Phys. Rev. B **96**, 174105 (2017).
[42]L. Wang, G. Walker, J. Chai, A. Iacopi, A. Fernandes, and S. Dimitrijev, Sci. Rep. **5**, 15423 (2015) and references therein.
[43]S. Karmann and R. Helbig, J. Appl. Phys. **66**, 3922 (1989).